

The Impact of Small-Angle Scattering on Ballistic Transport in Quantum Dots

A.M. See,¹ I. Pilgrim,² B.C. Scannell,² R.D. Montgomery,² O. Klochan,¹ A.M. Burke,¹ M. Aagesen,³ P.E. Lindelof,³ I. Farrer,⁴ D.A. Ritchie,⁴ R.P. Taylor,² A.R. Hamilton,¹ and A.P. Micolich¹

¹*School of Physics, University of New South Wales, Sydney NSW 2052, Australia*

²*Department of Physics, University of Oregon, Eugene, OR 97403-1274, USA*

³*Nanoscience Center, Niels Bohr Institute, University of Copenhagen,*

Universitetsparken 5, DK-2100 Copenhagen, Denmark

⁴*Department of Physics, Cavendish Laboratory, J. J. Thompson Avenue, Cambridge, CB3 0HE, United Kingdom*

(Dated: November 24, 2018)

Disorder increasingly affects performance as electronic devices are reduced in size. The ionized dopants used to populate a device with electrons are particularly problematic, leading to unpredictable changes in the behavior of devices such as quantum dots each time they are cooled for use. We show that a quantum dot can be used as a highly sensitive probe of changes in disorder potential, and that by removing the ionized dopants and populating the dot electrostatically, its electronic properties become reproducible with high fidelity after thermal cycling to room temperature. Our work demonstrates that the disorder potential has a significant, perhaps even dominant, influence on the electron dynamics, with important implications for ‘ballistic’ transport in quantum dots.

PACS numbers: 72.15.Qm, 73.63.-b, 75.70.Tj

Advances in semiconductor device technologies have enabled a long and fruitful study of nanoscale devices obtained by further confinement of the two-dimensional electron gas (2DEG) formed in an AlGaAs/GaAs heterostructure [1]. An important topic is ballistic transport effects, which are traditionally considered to occur when the large-angle scattering length exceeds the scale of additional confinement [2]. Following an early focus on fundamental phenomena such as the Aharonov-Bohm effect [3] and 1D conductance quantization [4, 5], the potential for novel devices was also explored [6]. A highlight with broad implications was the study of quantum chaos, where quantum dots were used as model dynamical systems called ‘billiards’ [7–10], alongside microwave [11], optical [12], acoustic [13] and cold atom systems [14]. The physics of wave chaos should be universal; however the various practical implementations differ, with important consequences for observed behavior [15], as we demonstrate for semiconductor billiards.

On its own, the large-angle scattering length ℓ , measured via the electron mobility, gives an incomplete picture of the overall electron scattering in an AlGaAs/GaAs heterostructure [16]. The 2DEG is normally populated by ionization of Si dopants, with high mobility obtained by spatially separating these dopants from the 2DEG. This ‘modulation doping’ [17] technique works because increases in dopant-2DEG separation convert the ionized dopants from large-angle to small-angle scattering sites that are effectively ‘hidden’ because the mobility is weighted towards large-angle scattering [16]. Nonetheless, the 2DEG still ‘feels’ the ionized dopants as a low-level ‘disorder potential’ with a length scale set by the 2DEG-donor separation [16, 18, 19]. This small-angle scattering length scale, typically of order 20–100 nm, is much smaller than both the typical quan-

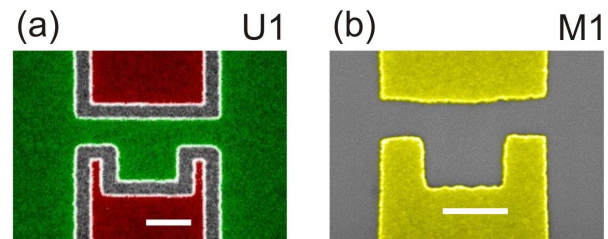


FIG. 1. (a/b) Scanning electron micrographs of undoped device U1 and modulation-doped device M1 with 500 nm scale bars (white). Green and red tinted regions in (a) indicate the n^+ GaAs top- and side-gates. Yellow tinted regions in (b) are Ti/Au gates on the heterostructure surface.

um dot width ($\sim 0.6 - 2 \mu\text{m}$) and the large-angle scattering length ($\sim 2 - 20 \mu\text{m}$). Although small-angle ionized dopant scattering was considered in early studies of quantum dot chaos [7, 20], it was generally expected to have little influence on transport. Scanning gate microscopy (SGM) allows direct visualization of electron flow in nanoscale devices [19, 21, 22], and small-angle scattering clearly causes significant deviations from the straight trajectories envisioned in the ballistic transport paradigm [2, 8, 10]. This raises two important questions: What is the true impact of small-angle scattering on transport, as measured by the conductance, in quantum dots? Can its effect be reduced or eliminated?

We address both questions by measuring the low temperature magnetoconductance $G(B)$ of two quantum dots (Fig. 1) with nominally identical geometry, one on undoped (U1) and one on modulation-doped (M1) heterostructure, before and after thermal cycling to room temperature. Our undoped dot design evolved from the Heterostructure Insulated Gate Field-Effect Transis-

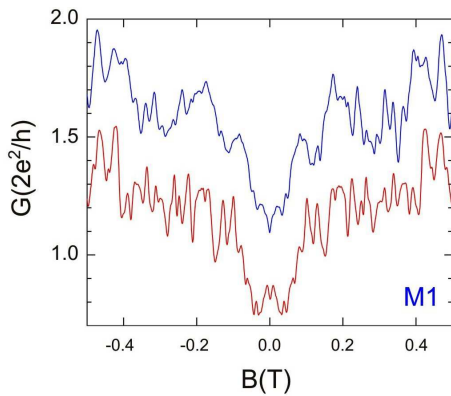


FIG. 2. Magnetoconductance $G(B)$ vs perpendicular magnetic field B for M1 with $V_{SG} = -443.5$ mV before (blue) and after (red) thermal cycling to $T = 300$ K. The red trace is vertically offset by -0.6 for clarity.

tor (HIGFET) conceived by Solomon *et al* [23]. The heterostructure consists of an undoped GaAs substrate overgrown with 160 nm undoped AlGaAs, 25 nm undoped GaAs, and a 35 nm n^+ GaAs cap. The cap is highly conductive at low temperature and divided into three independently biasable gates (Fig. 1(a)). A positive bias $V_{TG} > 0.32$ V applied to the top-gate (green) electrostatically populates the dot and source and drain reservoirs. A negative voltage V_{SG} applied to the side-gates (red) tunes the dot area and width of the quantum point contacts (QPCs) connecting the dot to source and drain. A mobility $\mu \sim 300,000$ cm^2/Vs is obtained at $n \sim 1.8 \times 10^{11}$ cm^{-2} , corresponding to $\ell \sim 2.1$ μm . The modulation-doped heterostructure has $\mu \sim 333,000$ cm^2/Vs at $n \sim 2.4 \times 10^{11}$ cm^{-2} giving $\ell \sim 2.7$ μm . The 2DEG-dopant separation is 20 nm, as in [7], where comparable mobility is obtained. M1 is defined by side-gates (Fig. 1(b)) negatively biased to $V_{SG} < -0.23$ V, more negative V_{SG} decreases the dot area and QPC width. Further details on the undoped devices are available elsewhere [24–27].

Electrical measurements were performed in the dark at a temperature $T \sim 230$ mK, with $G(B)$ obtained by standard four-terminal lock-in techniques with the magnetic field B perpendicular to the 2DEG. The low temperature $G(B)$ shows quantum interference fluctuations [28] that provide a ‘magnetofingerprint’ [29] of the distribution of electron trajectories through the dot. Note that in addition to dot geometry, $G(B)$ is highly sensitive to the disorder distribution [29]. To isolate the effect small-angle scattering has on transport, we examine the changes in $G(B)$ induced by thermal cycling of dots with and without modulation doping. This relies on the well-known tendency for the disorder potential to differ between cooldowns in modulation-doped $\text{Al}_x\text{Ga}_{1-x}\text{As}$ heterostructures with $x \gtrsim 0.22$ due to the capture of excess electrons by deep donors known as DX centres

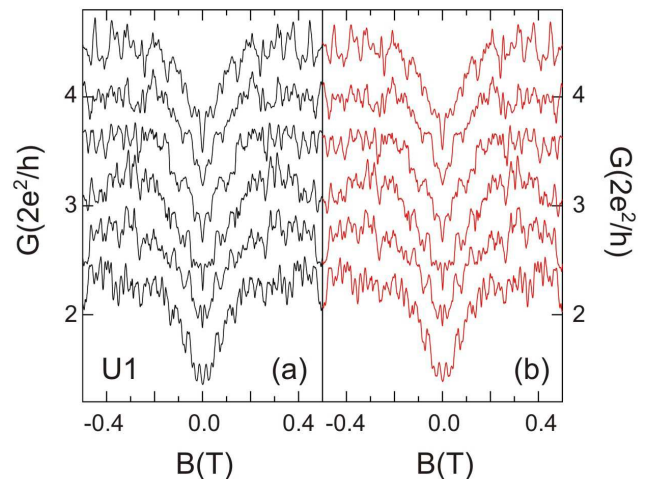


FIG. 3. $G(B)$ vs B for U1, increasing V_{TG} from +930 mV (top) to +955 mV (bottom) in 5 mV steps, (a) before (black) and (b) after (red) thermal cycling to $T = 300$ K.

[30, 31]. In modulation-doped devices, this leads to significant changes in $G(B)$ upon warming above $T \sim 150$ K despite the defined dot geometry remaining exactly the same [32, 33], as shown in Fig. 2, where we plot $G(B)$ for device M1 before and after thermal cycling to $T = 300$ K. Many attempts were made to obtain reproducible $G(B)$ traces from M1 without success [24].

Figure 3(a/b) presents $G(B)$ data from the first and second cooldowns of device U1, with side-by-side comparisons for six different V_{TG} . Remarkably, $G(B)$ is reproducible with high-fidelity in U1 despite thermal cycling to room temperature, in stark contrast to modulation-doped devices. We observe this behavior in other undoped devices and for repeated cooldowns of a single undoped device [24]. We used a cross-correlation analysis to quantify the extent of changes in $G(B)$ due to thermal cycling, with the correlation F normalized to give $F = 1$ ($F = 0$) for identical (randomly-related) traces [24, 34]. We obtain $F = 0.94$ for the upper two U1 data traces in Fig. 3(a/b) ($V_{TG} = +930$ mV), compared to a maximum of $F = 0.75$ for M1, mostly due to the similar $G(B)$ background [24].

The fact that $G(B)$ is reproducible after thermal cycling for U1 but not for M1 demonstrates that the ionized dopant disorder potential has a significant, perhaps even dominant, influence on the electron dynamics. It immediately shows that small-angle scattering cannot be ignored and that the commonly-held simplistic picture of electrons following straight-line trajectories that undergo specular reflections at the dot walls is unrealistic. The question is, how does this affect our understanding of electron transport in quantum dots? Two aspects are involved here: length scale and the effect on experimental signatures of the dynamics.

Dealing with length scale first; from a semiclassical

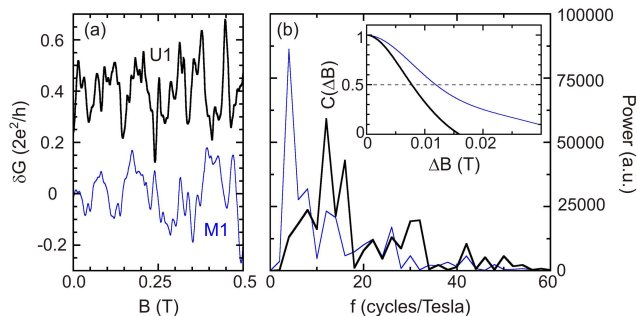


FIG. 4. (a) Extracted magnetoconductance fluctuations δG vs B for U1 (uppermost left trace in Fig. 3 – thick black line) and M1 (uppermost trace in Fig. 2 – thin blue line). The U1 data is vertically offset by +0.4 for clarity. (b) Fourier power spectra and (inset) normalized autocorrelation functions obtained for the two traces in (a).

view, ignoring disorder, there is a wide distribution of lengths in the set of all possible electron trajectories within the dot that intercept the QPCs and thus contribute to $G(B)$ [35]. One can naturally expect that the impact of small-angle scattering to increase with trajectory length, being minimal for the shortest trajectories. SGM studies of dots show clear evidence that shorter ballistic trajectories survive the diffusive effect of small-angle scattering [36, 37]. This suggests that studies focussed on the influence of short periodic orbits on $G(B)$ spectral content [38] may be robust, partly due to the reduced impact of small-angle scattering for short trajectories, but perhaps also because quantum interference may enable these orbits to survive despite the diffusive effect of small-angle scattering [37, 39, 40]. Regarding longer paths, the difficulty is that $G(B)$ reflects the distribution of areas enclosed by possible trajectories, and this does not directly map to the trajectory length distribution due to flux-cancellation effects [41]. Thus changes in disorder potential will impact broadly across the spectrum of $G(B)$ fluctuations. One case where longer paths may be more robust to the disorder potential are skipping orbits running along the dot walls at moderate B [42]. These may be reinforced by the process described by Büttiker (see Fig. 4 of [43]). The feasibility of this is evident in the SGM studies by Aidala *et al* [22].

To demonstrate that small-angle scattering has a tangible effect on the statistics of $G(B)$ fluctuations, in Fig. 4(b) we present Fourier power spectra and autocorrelation analyses of representative data from U1 and M1 (Fig. 4(a)); we obtain qualitatively similar results for other traces (see Fig. S3 in [24]). The fluctuations are extracted by symmetrizing the data, and removing a third-order polynomial fit as per [7]. The rms amplitudes are similar (0.0985 and $0.0925 \times 2e^2/h$ for U1 and M1), but higher frequency fluctuations are clearly evident for U1. This is borne out in Fig. 4(b), where

the U1 spectra shows enhanced power at higher frequencies relative to M1, confirmed by the autocorrelation analysis [7, 8] inset to Fig. 4(b). The correlation $C(\Delta B) = \langle \delta G(B) \delta G(B + \Delta B) \rangle$ drops more rapidly for U1, consistent with richer structure in the fluctuations (the correlation fields for U1 and M1 are 7.8 and 11.9 mT). An interesting aspect of Fig. 4(b) is a distinct tendency towards a higher frequency for the dominant peak in the U1 spectra; this may point directly to the influence of disorder on transport given that U1 and M1 have nominally identical geometry and differ in the presence/absence of small-angle ionized dopant scattering.

Turning now to how small-angle scattering affects experimental signatures of the electron dynamics, the most obvious is $G(B)$ itself. Berry *et al* [44] proposed that $G(B)$ could be directly used as a magnetofingerprint to detect the change in electron dynamics induced by adding a narrow barrier to the interior of a circular quantum dot. This required two separate devices, and our findings show that an equivalent change in $G(B)$ would have resulted from room temperature thermal cycling of either of these modulation-doped devices. The same problem exists for more recent work also, e.g., [45]. Simple statistical measures are also affected; for example, Fig. 3 of Marcus *et al* [7] presents power spectra for two separate nominally identical device ‘chips’, each containing one circular and one stadium-shaped dot. If small-angle scattering from the disorder potential was negligible, one would expect the power spectra for the circular dot on each chip to be very similar, the same should hold for the two stadia. Indeed, differences in spectra between stadium and circle are no more or less substantial than those between two identical dot geometries in Fig. 3 of [7]. This suggests these spectral differences are not due to geometry alone but also reflect differences in disorder potential (e.g. see Fig. S4 of [24]).

It is important to note that in both cases above we do not claim that dot geometry has no effect on electron dynamics at all, only that small-angle scattering masks its effect on $G(B)$ as an experimental signature of dynamics. One approach that may overcome the effect of small-angle scattering is that used by Chang *et al* [9], where a 6×8 array of nominally identical dots was measured to average out the $G(B)$ fluctuations. Our findings suggest this essentially constitutes an averaging of the dot disorder potentials to expose the effect of the common lithographic geometry. Although the link between zero-field conductance peak lineshape and dynamics has been questioned [46, 47], this dot array approach may be useful for comparing other aspects of the measured $G(B)$ to theoretical predictions, providing the array of dots is sufficiently identical lithographically. Such studies would be aided considerably by the undoped device architecture [23, 25, 27]. More complex spectral analyses involving significant post-measurement averaging of $G(B)$ fluctuations may also be helpful.

Although removal of modulation doping significantly reduces small-angle scattering, we expect substantial disorder to remain, e.g., background impurities, interface roughness. It is difficult to comment further on this remnant disorder, but our data shows that it is robust to thermal cycling. We suspect this remnant disorder will prevent perfectly identical $G(B)$ from being obtained in separate, nominally-identical undoped devices, obviating the truly ballistic quantum dots envisioned theoretically [8, 10], but the considerably improved thermal robustness of our undoped architecture, along with the ability to reduce *both* large- and small-angle scattering, makes it highly appealing towards potential practical applications of ballistic transport devices [6].

Our results also have more broad implications for our understanding of disorder in mesoscopic devices, highlighting the limitations of mobility as a metric for disorder. For example, some may argue that HIGFETs failed to meet expectations because the highest mobilities obtained fall short of those in modulation-doped structures. We believe this belies the truth, because as pointed out earlier, the mobility is heavily weighted towards large-angle scattering [16], and hence small-angle scattering is more or less ignored considering mobility alone. The fact that small-angle scattering has a major effect on transport at length scales much smaller than expected from the mobility (i.e., at the ~ 20 nm scale rather than ~ 2000 nm) is evident in both SGM studies [19, 22] and the lack of $G(B)$ reproducibility under thermal cycling in modulation-doped dots. The importance of this broader picture of disorder is also evident in very recent studies of the $5/2$ fractional quantum Hall state [48], driven by interest in the $5/2$ state for topological quantum computation, and the associated need for ultra-low disorder heterostructures. From this perspective, we suggest the $G(B)$ in quantum dots may be highly useful for detecting changes in the small-angle scattering potential whilst studying scattering mechanisms in high-mobility modulation-doped heterostructures [49]. Alternatively, shallow dots in inverted undoped heterostructures [50] might be used to detect changes in charge environment at or above the heterostructure surface; for example; using chemical treatments between thermal cycles may aid the study of surface charge effects on transport [51], or enable dots to be used for charge detection more generally. Dopant reconfiguration is also a well known source of charge noise in modulation-doped devices [52]; our undoped devices' thermal robustness suggests they may offer a path to devices with significantly reduced charge noise.

This work was funded by the Australian Research Council (ARC) [DP0772946, LX0882222, FT0990285], Office of Naval Research [N00014-07-0457], US Air Force [FA8650-05-1-5041], National Science Foundation and Research Corporation, and performed using the Australian National Fabrication Facility. APM/ARH ac-

knowledge ARC Future/Professorial Fellowships.

-
- [1] D.K. Ferry, S.M. Goodnick and J.P. Bird, *Transport in Nanostructures* 2nd Ed., (Cambridge University Press, Cambridge, 2009).
 - [2] C.W.J. Beenakker and H. van Houten, *Solid State Physics* **44**, 1 (1991).
 - [3] G. Timp *et al.*, *Phys. Rev. Lett.* **58**, 2814 (1987).
 - [4] B.J. van Wees *et al.*, *Phys. Rev. Lett.* **60**, 848 (1988).
 - [5] D.A. Wharam *et al.*, *J. Phys. C* **21**, L209 (1988).
 - [6] S.M. Goodnick and J.P. Bird, *IEEE Trans. Nanotech.* **2**, 368 (2003).
 - [7] C.M. Marcus, A.J. Rimberg, R.M. Westervelt, P.F. Hopkins and A.C. Gossard, *Phys. Rev. Lett.* **69**, 506 (1992).
 - [8] R.A. Jalabert, H.U. Baranger and A.D. Stone, *Phys. Rev. Lett.* **65**, 2442 (1990).
 - [9] A.M. Chang, H.U. Baranger, L.N. Pfeiffer and K.W. West, *Phys. Rev. Lett.* **73**, 2111 (1994).
 - [10] R.V. Jensen, *Nature* **355**, 311 (1992); *Nature* **373**, 16 (1995).
 - [11] H.-J. Stöckmann and J. Stein, *Phys. Rev. Lett.* **64**, 2215 (1990).
 - [12] C. Gmachl *et al.*, *Science* **280**, 1556 (1998).
 - [13] K. Schaadt, A.P.B. Tufaile and C. Ellegaard, *Phys. Rev. E* **67**, 026213 (2003).
 - [14] C. Zhang, J. Liu, M.G. Raizen and Q. Niu, *Phys. Rev. Lett.* **93**, 074101 (2004).
 - [15] K.-F. Berggren and Z.-L. Ji, *Chaos* **6**, 543 (1996).
 - [16] P.T. Coleridge, *Phys. Rev. B* **44**, 3793 (1991).
 - [17] R. Dingle, H.L. Störmer, A.C. Gossard and W. Wiegmann, *Appl. Phys. Lett.* **78**, 665 (1978).
 - [18] J.A. Nixon and J.H. Davies, *Phys. Rev. B* **41**, 7929 (1990).
 - [19] M.P. Jura *et al.*, *Nature Physics* **3**, 841 (2007).
 - [20] W.A. Lin, J.B. Delos and R.V. Jensen, *Chaos* **3**, 655 (1993).
 - [21] M.A. Topinka *et al.*, *Nature* **410**, 183 (2001).
 - [22] K.E. Aidala *et al.*, *Nature Physics* **3**, 464 (2007).
 - [23] P.M. Solomon, C.M. Knoedler and S.L. Wright, *IEEE Electron Dev. Lett.* **5**, 379 (1984).
 - [24] See EPAPS Document No. E-PRLTAO-XX-XXXXXX for 4 supplementary figures, and extended discussion of the methods. For more information on EPAPS, see <http://www.aip.org/pubservs/epaps.html>.
 - [25] B.E. Kane, L.N. Pfeiffer, K.W. West and C.K. Harnett, *Appl. Phys. Lett.* **63**, 2132 (1993).
 - [26] W.R. Clarke, A.P. Micolich, A.R. Hamilton, M.Y. Simmons, K. Muraki and Y. Hirayama, *J. Appl. Phys.* **99**, 023707 (2006).
 - [27] A.M. See, O. Klochan, A.R. Hamilton, A.P. Micolich, M. Aagesen and P.E. Lindelof, *Appl. Phys. Lett.* **96**, 112104 (2010).
 - [28] A.D. Stone, *Phys. Rev. Lett.* **54**, 2692 (1985).
 - [29] S. Feng, P.A. Lee and A.D. Stone, *Phys. Rev. Lett.* **56**, 1960 (1986).
 - [30] P.M. Mooney, *J. Appl. Phys.* **67**, R1 (1990); *Semicond. Sci. Technol.* **6**, B1 (1991).
 - [31] A.R. Long *et al.*, *Semicond. Sci. Technol.* **8**, 1581 (1993).
 - [32] B.C. Scannell *et al.*, arXiv:1106.5823 (2011).
 - [33] C. Berven, M.N. Wybourne, A. Ecker and S.M. Good-

- nick, Phys. Rev. B **50**, 14639 (1994).
- [34] R.P. Taylor, A.P. Micolich, R. Newbury and T.M. Fromhold, Phys. Rev. B **56**, R12733 (1997).
- [35] H.U. Baranger, R.A. Jalabert and A.D. Stone, Chaos **3**, 665 (1993).
- [36] R. Crook, C.G. Smith, A.C. Graham, I. Farrer, H.E. Beere and D.A. Ritchie, Phys. Rev. Lett. **91**, 246803 (2003).
- [37] A.M. Burke, R. Akis, T.E. Day, G. Speyer, D.K. Ferry and B.R. Bennett, Phys. Rev. Lett. **104**, 176801 (2010).
- [38] J.P. Bird *et al.*, Phys. Rev. Lett. **82** 4691 (1999).
- [39] I.V. Zozoulenko, R. Schuster, K.-F. Berggren and K. Ensslin, Phys. Rev. B **55**, 10209 (1997).
- [40] E.J. Heller, Phys. Rev. Lett. **53**, 1515 (1984).
- [41] C.W.J. Beenakker and H. van Houten, Phys. Rev. B **37**, 6544 (1988).
- [42] L. Christensson, H. Linke, P. Omling, P.E. Lindelof, I.V. Zozoulenko and K.-F. Berggren, Phys. Rev. B **57**, 12306 (1998).
- [43] M. Büttiker, Phys. Rev. B **38**, 9375 (1988).
- [44] M.J. Berry, J.A. Katine, R.M. Westervelt and A.C. Gosard, Phys. Rev. B **50**, 17721 (1994).
- [45] A.P. Micolich *et al.*, Phys. Rev. B **70**, 085302 (2004).
- [46] J.P. Bird *et al.*, Phys. Rev. B **52**, R14336 (1995).
- [47] R. Akis, D.K. Ferry, J.P. Bird and D. Vasileska, Phys. Rev. B **60**, 2680 (1999).
- [48] W. Pan *et al.*, Phys. Rev. Lett. **106**, 206806 (2011).
- [49] D. Laroche, S. Das Sarma, G. Gervais, M.P. Lilly and J.L. Reno, Appl. Phys. Lett. **96**, 162112 (2010).
- [50] U. Meirav, M. Heiblum and F. Stern, Appl. Phys. Lett. **52**, 1268 (1986).
- [51] W.Y. Mak, K. Das Gupta, H.E. Beere, I. Farrer, F. Sfigakis and D.A. Ritchie, Appl. Phys. Lett. **97**, 242107 (2010).
- [52] C. Buizert *et al.*, Phys. Rev. Lett. **101**, 226603 (2008).